

## Supporting Information

### **Imparting hydrophobicity to MOF on Layered MXene for the selective, rapid, and ppb level humidity-independent detection of NH<sub>3</sub> at room temperature**

*Kugalur Shanmugam Ranjith<sup>a</sup>, Sonam Sonwal<sup>b</sup>, Ali Mohammadi<sup>a</sup>, Ganji Seeta Rama Raju<sup>a</sup>, Mi-Hwa Oh<sup>c</sup>, Yun Suk Huh<sup>b,\*</sup>, Young-Kyu Han<sup>a,\*</sup>*

<sup>a</sup>Department of Energy and Material Engineering, Dongguk University-Seoul, Seoul 04620, Republic of Korea

<sup>b</sup>Department of Biological Engineering, Inha University, Incheon 22212, Republic of Korea

<sup>c</sup>National Institute of Animal Science, Rural Development Administration, Wanju 55365, Republic of Korea

\*Corresponding authors: yunsuk.huh@inha.ac.kr (Y. S. Huh), ykenergy@dongguk.edu (Y.-K. Han)

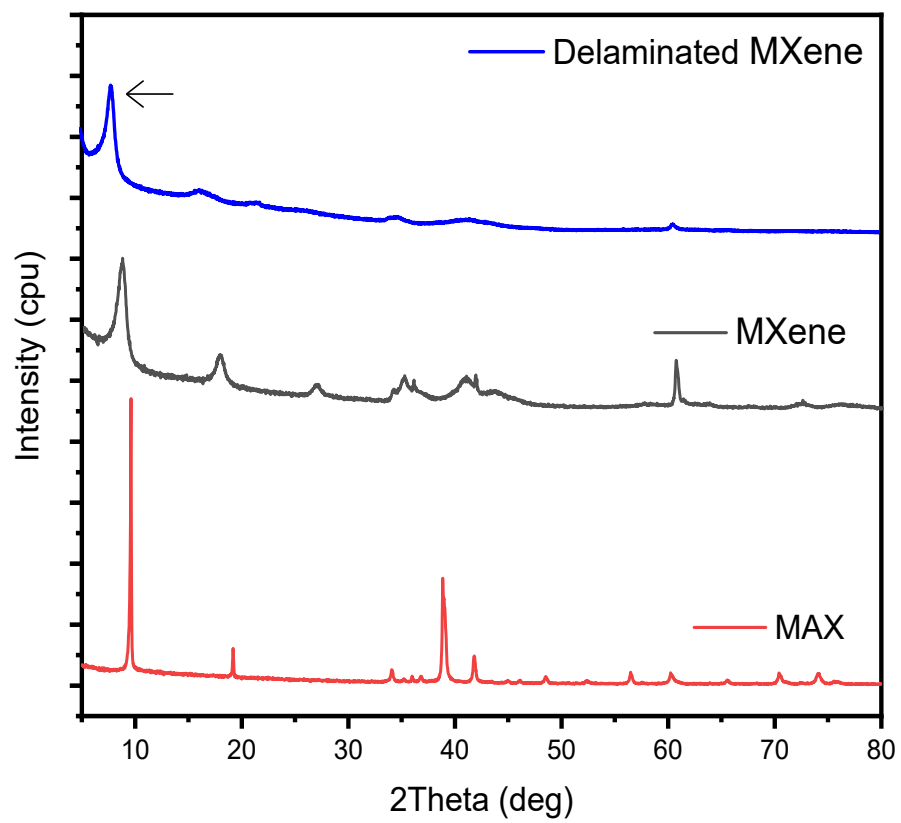


**Fig. S1** The XRD spectrum of MAX, MXene and delaminated MXene.

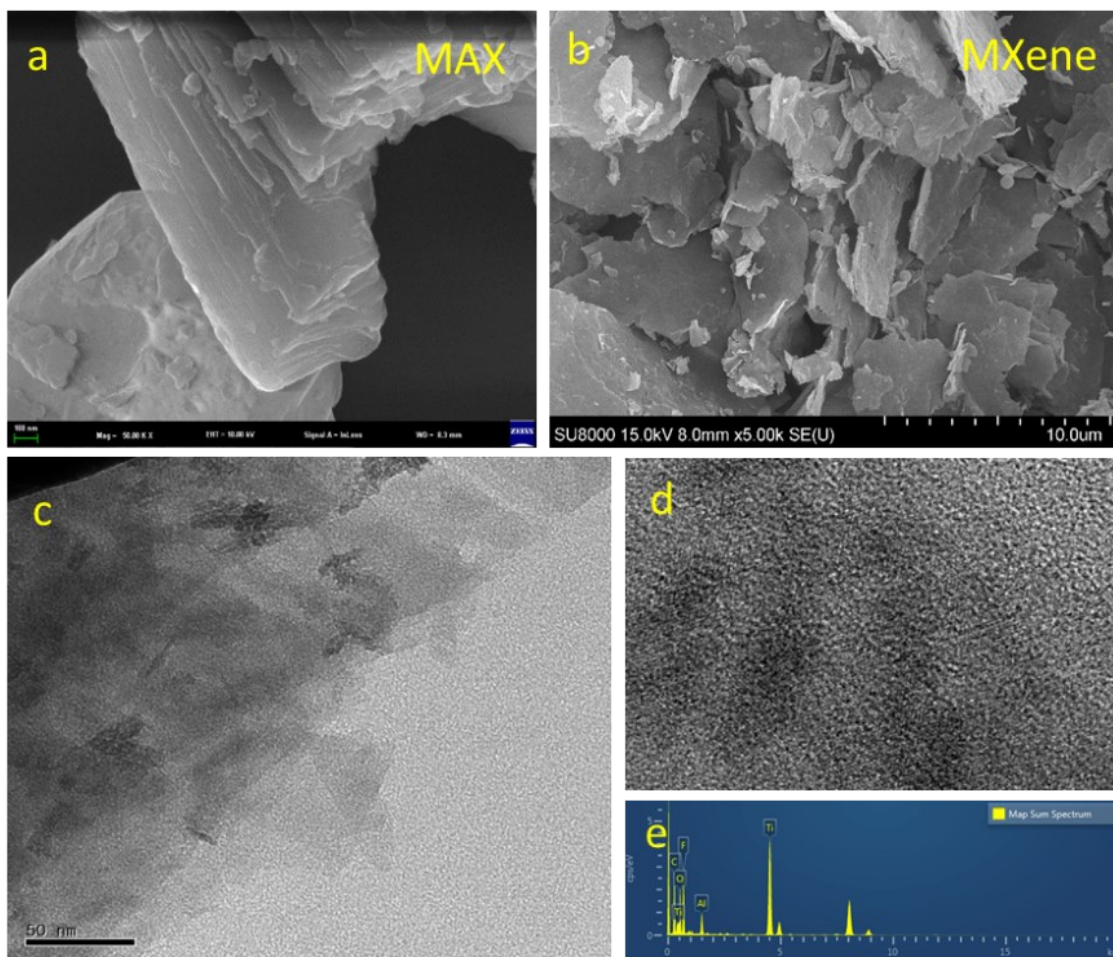


**Fig. S2** SEM of (a) MAX and (b) MXene. (c-e) TEM images and EDAX spectra of the MXene nanosheets.

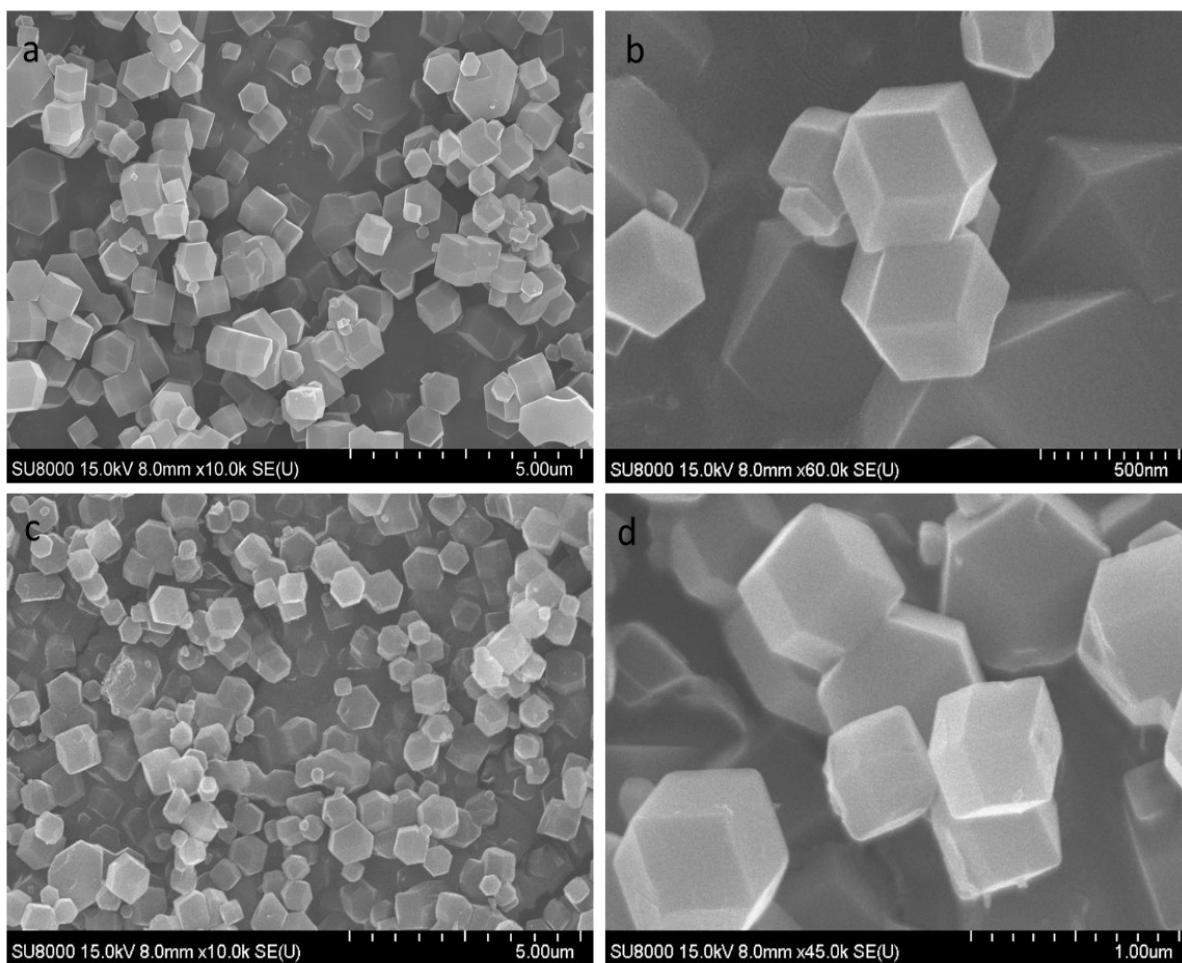


**Fig. S3** SEM images of (a, b) ZIF-67 and (c, d) H-ZIF-67 nanostructures.

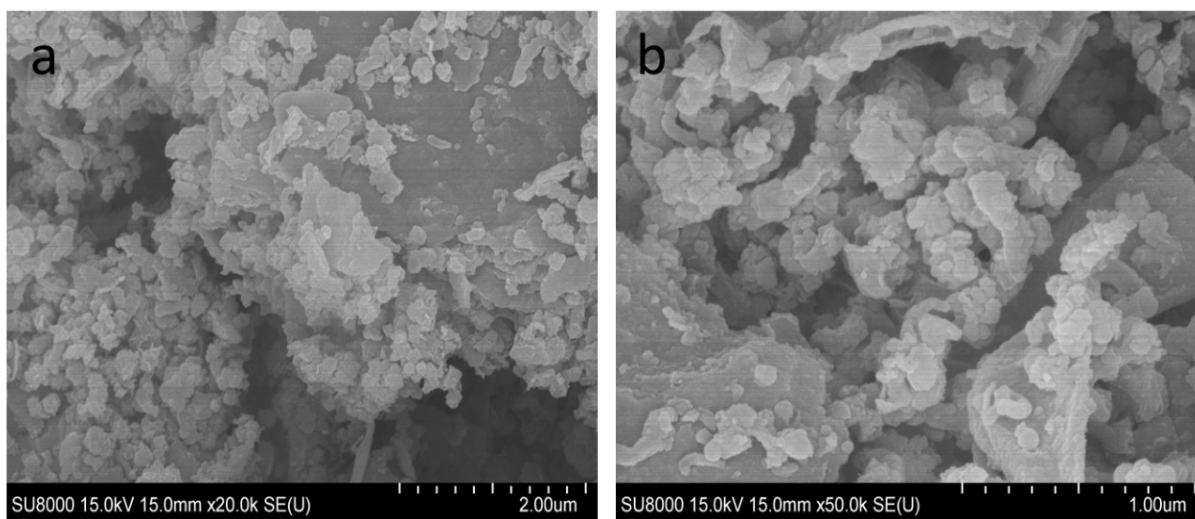


**Fig. S4** SEM of ZIF/MXene composite without nucleation process.

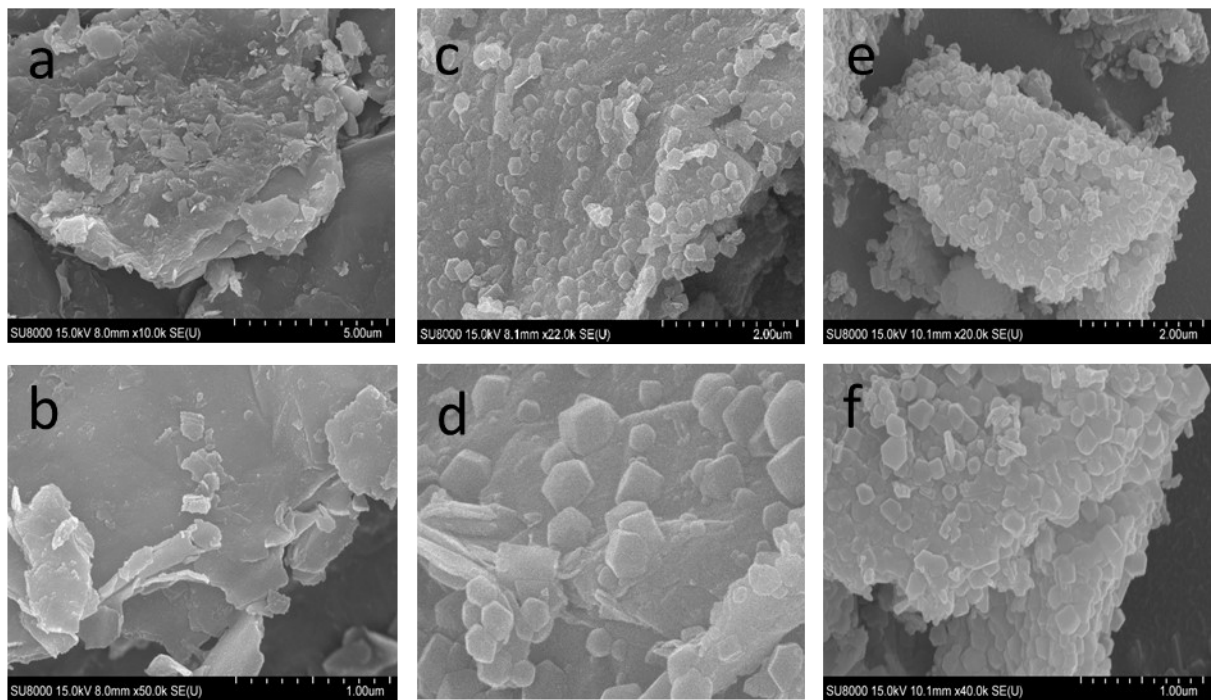


**Fig. S5** SEM images of MOF loading density on MXene (a, b) 2 wt.% (c, d) 6 wt.% and (e, f) 10 wt.%.

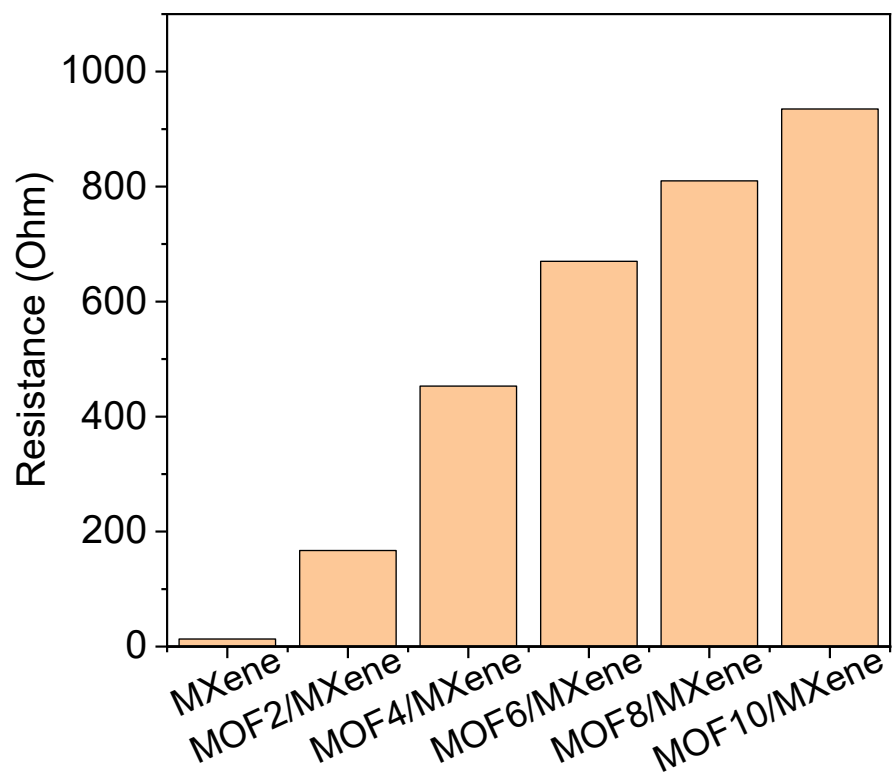


**Fig. S6** Resistance of the different densities of MOF-loaded MXene at the potential difference of 1V.

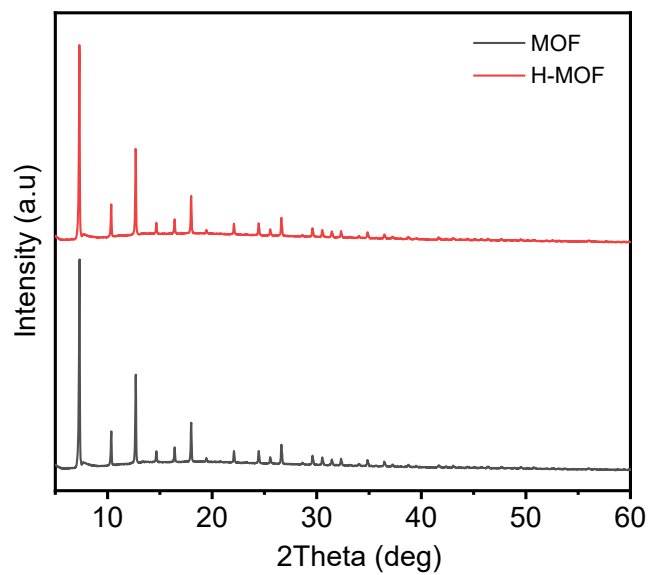


**Fig. S7** XRD spectrum of MOF (ZIF-67) and H-ZIF (H-ZIF-67) nanostructures.



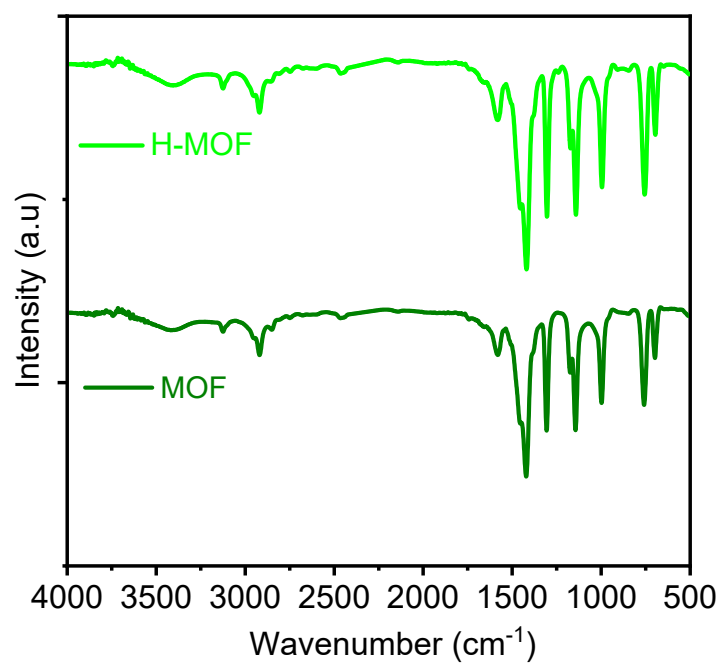


**Fig. S8** FTIR spectrum of MOF and H-MOF nanostructures.

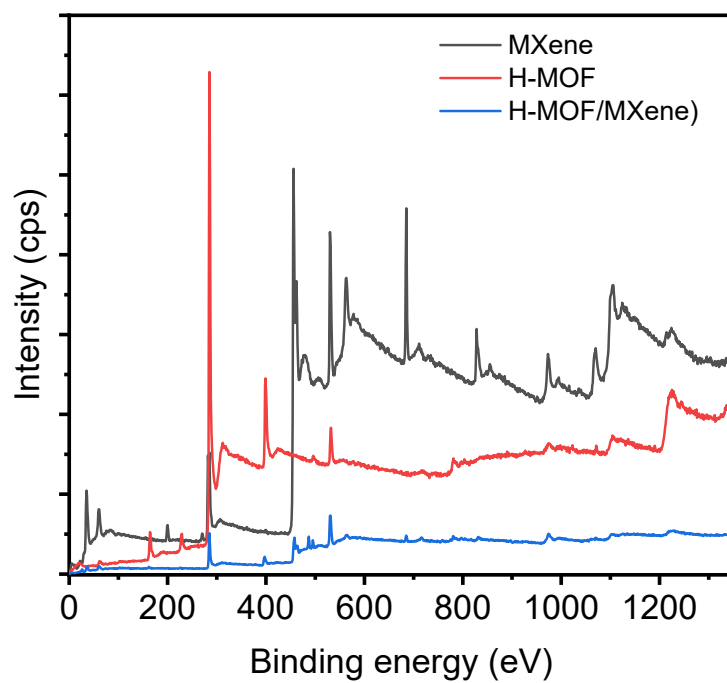


**Fig. S9** XPS survey spectrum of MXene, H-MOF, and H-MOF/MXene heterostructures.

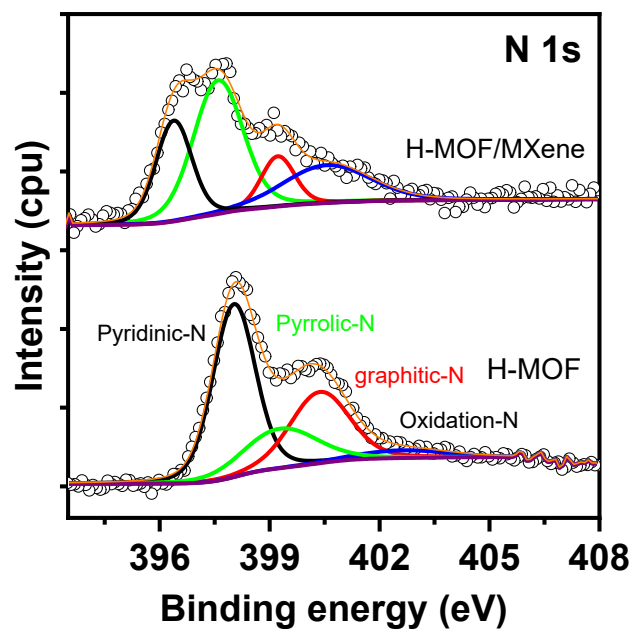


**Fig. S10** N 1s XPS spectrum of H-MOF and H-MOF/MXene samples.

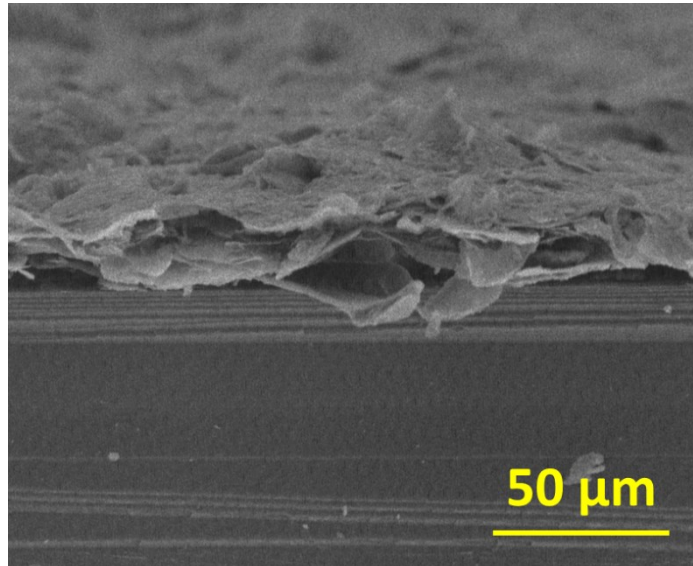


**Fig. S11** Cross sectional SEM image of fabricated MXene-based sensor on the IDE electron coated on SiO<sub>2</sub> substrate.

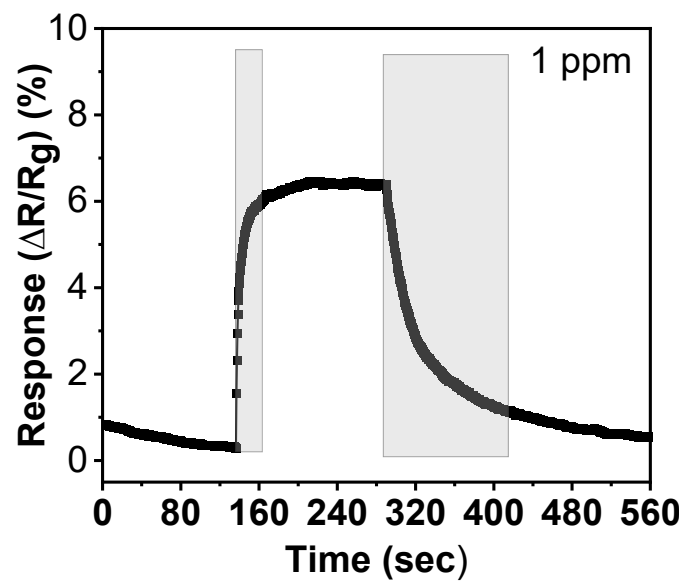


**Fig. S12** Response and recovery graph of the H-MOF<sub>6</sub>/MXene hybrid sample.

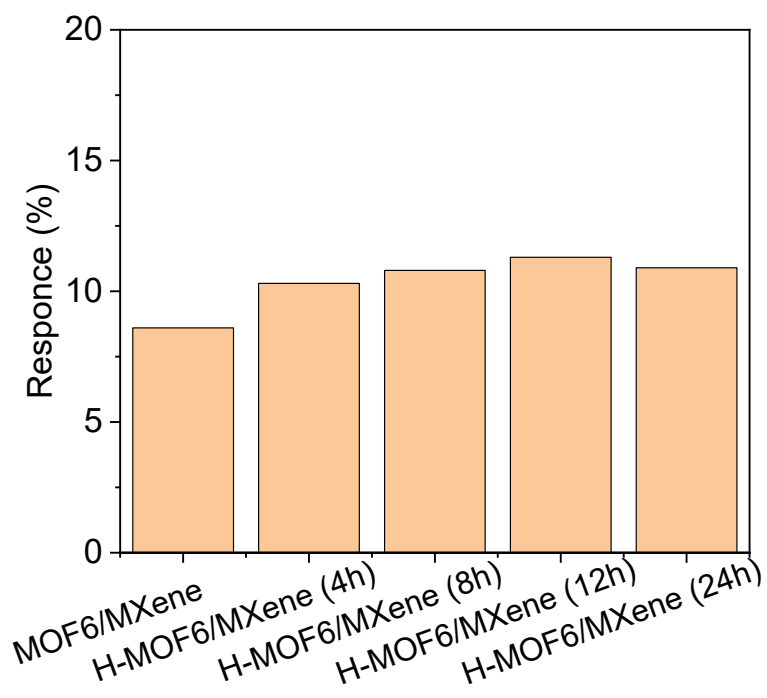


**Fig. S13** Response graph of the H-MOF<sub>6</sub>/MXene hybrid samples with the function of different immersion times of DMBIM over the MOF/MXene hybrid.

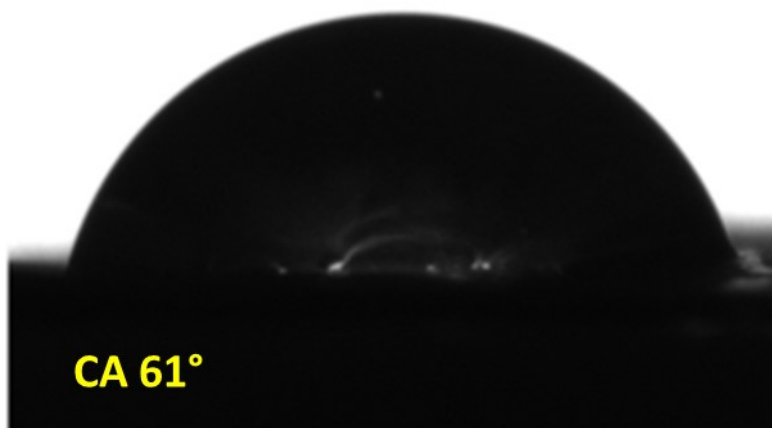


**Fig. S14** Contact angle measurement of the pristine MXene sample.

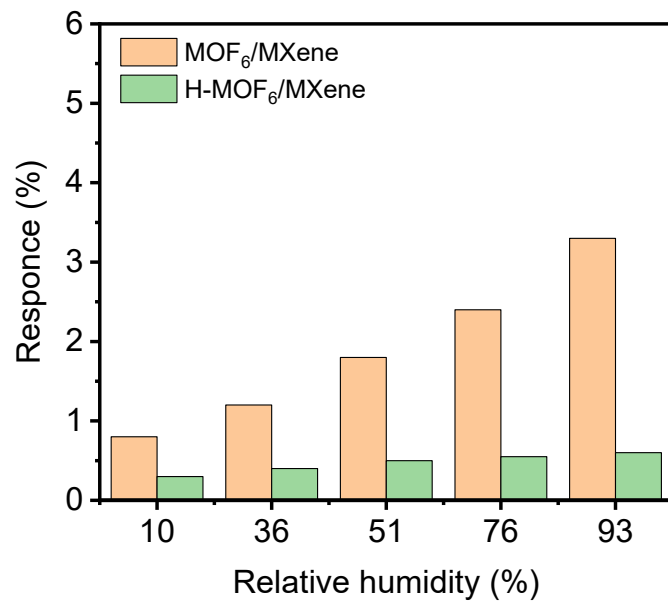


**Fig. S15** Humidity response of the MOF<sub>6</sub>/MXene and H-MOF<sub>6</sub>/MXene sensors.



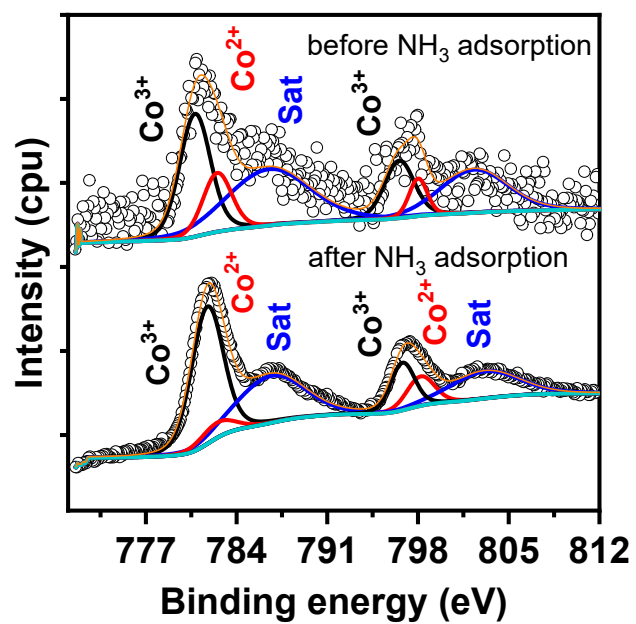


**Fig. S16** Co 2p XPS spectra of the H-MOF<sub>6</sub>/MXene hybrid before and after the NH<sub>3</sub> absorption.

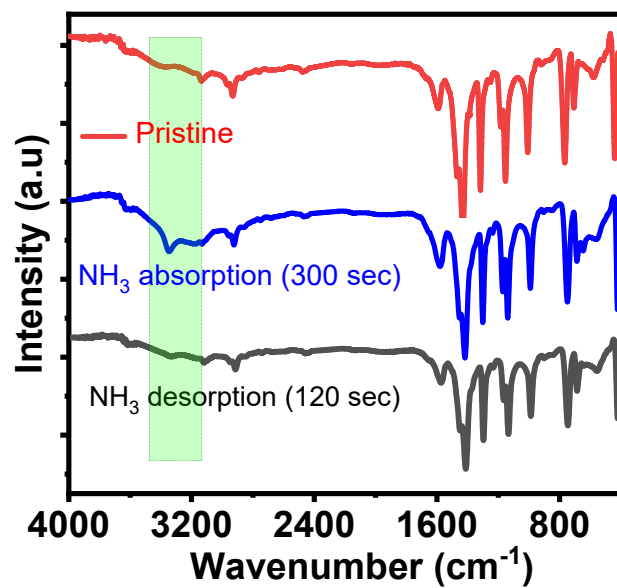


**Fig. S17** FTIR spectra of the H-MOF/MXene sample with the function of NH<sub>3</sub> adsorption and desorption nature over time.

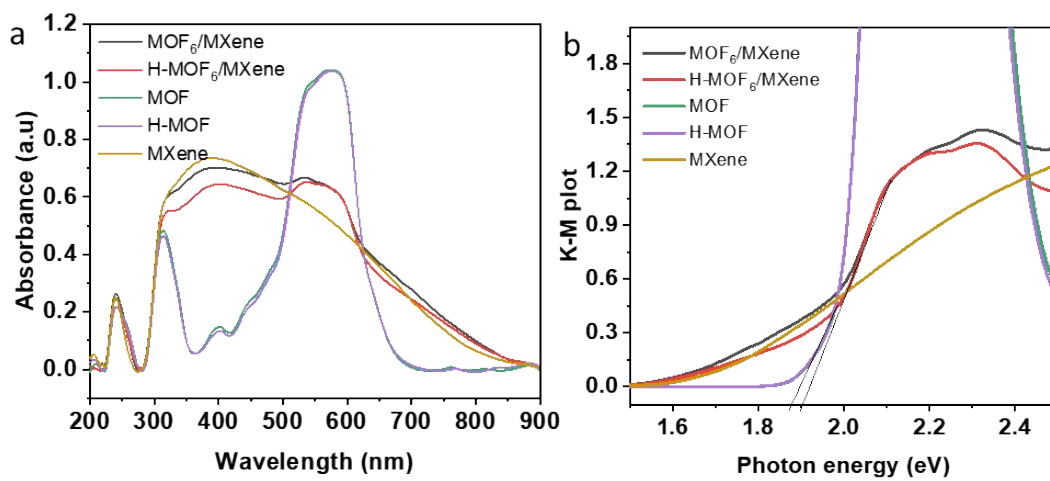


**Fig. S18** (a) UV-DRS spectra and (b) K-M plot of the MXene-based hybrid samples.

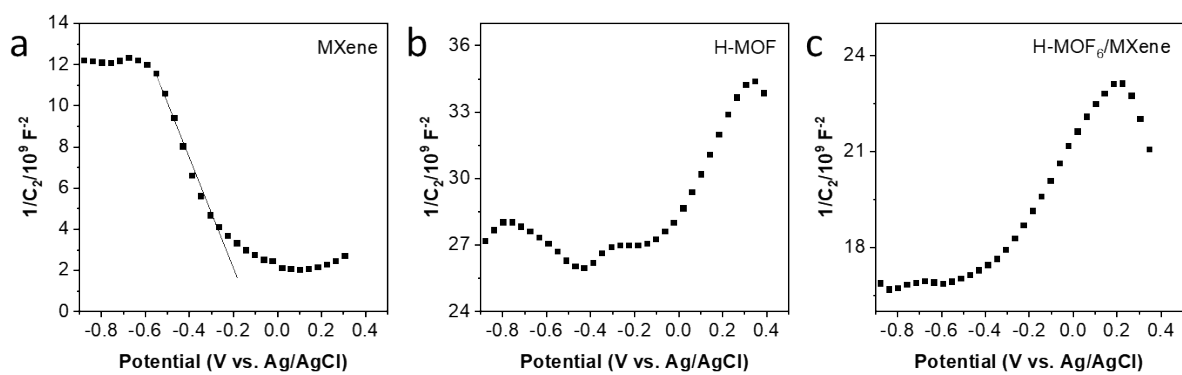


**Fig. S19** Mott-Schottky plot for the (a) MXene, (b) H-MOF, and (c) H-MOF<sub>6</sub>/MXene-based nanostructures.

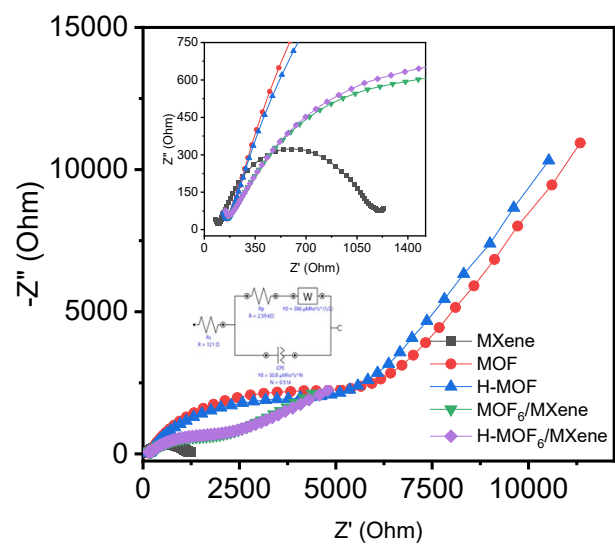


**Fig. S20** EIS spectra of the MXene-based hybrid samples.